IEEE Photonics Journal
An IEEE Photonics Society Publication

Open Access

Experimental Study of the Refractive Index Sensitivity in Arc-induced Long Period Gratings

Volume 9, Number 1, February 2017

Flavio Esposito
Rajeev Ranjan
Stefania Campopiano
Agostino Iadicicco

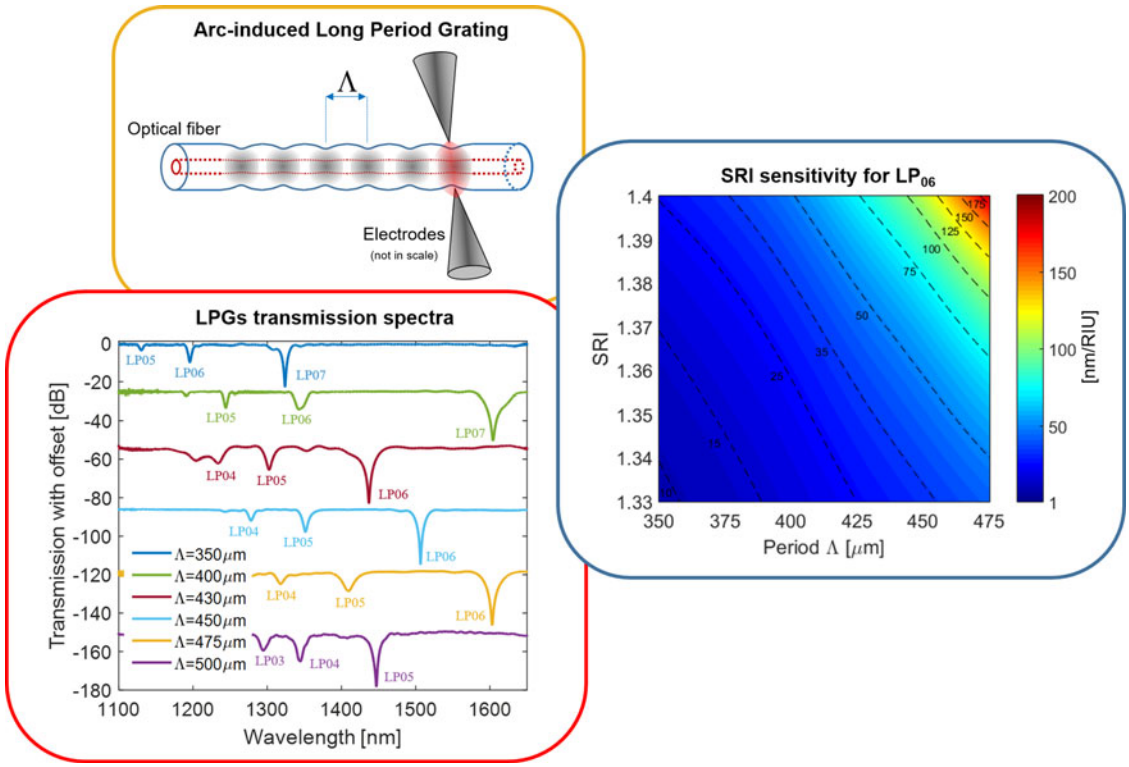

DOI: 10.1109/JPHOT.2016.2634784
1943-0655 © 2016 IEEE

IEEE photonics SOCIETY

IEEE

Experimental Study of the Refractive Index Sensitivity in Arc-induced Long Period Gratings

Flavio Esposito, Rajeev Ranjan, Stefania Campopiano, and Agostino Iadicicco

Department of Engineering, University of Naples "Parthenope," Centro Direzionale Isola C4, Naples, 80143, Italy

DOI:10.1109/JPHOT.2016.2634784

Manuscript received November 2, 2016; revised November 26, 2016; accepted November 28, 2016. Date of publication December 1, 2016; date of current version December 21, 2016. This work was supported by the Italian Ministry of Education, University, and Research through the funded project "Tecnologie optoelettroniche innovative per il monitoraggio e la diagnostica dell'infrastruttura ferroviaria" (OPTOFER PON03PE_00155_1) (D.M. 593/2000). Corresponding author: A. Iadicicco (e-mail: iadicicco@uniparthenope.it).

Abstract: This paper presents an experimental study of the sensitivity characteristics to the surrounding refractive index (SRI) in arc-induced long period gratings (LPGs), in order to outline their dependence over the fabrication parameters. Several LPGs were fabricated, with spectral features that are appealing for chemical sensing applications, e.g., negligible power losses, bands depth greater than 20 dB, and total length smaller than 35 mm. In addition, low spatial periods Λ, which are close to the limit of the arc-based fabrication technique, were selected in order to excite high-order cladding modes. In particular, the period was chosen in range 350–500 μm to focus attention on the same cladding modes for the gratings under investigation. Accordingly, a wide experimental analysis was then carried out to investigate the dependence of the sensitivity to SRI changes on the period in order to derive design criteria for LPG fabrication. In the wavelength range 1100–1700 nm and taking into consideration the attenuation bands related to the LP_{05} and LP_{06} cladding modes, an SRI sensitivity enhancement up to one order of magnitude can be achieved by proper selection of the grating period.

Index Terms: Fiber gratings, waveguide devices, sensors.

1. Introduction

Long period gratings (LPGs) are in-fiber devices, which rely on coupling the light from the fundamental core mode of a single mode fiber to cladding modes, with the result that one or more attenuation bands are visible in the fiber transmission spectrum. These bands are positioned at the wavelengths $\lambda_{res,i}$ [1], [2], satisfying the phase-matching condition

$$\lambda_{res,i} = (n_{eff,co} - n_{cl,i}) \cdot \Lambda \tag{1}$$

where $n_{eff,co}$ and $n_{cl,i}$ are, respectively, the effective refractive index of the core and of the ith cladding mode, whereas Λ is the grating spatial period. These devices were first introduced by Vengsarkar *et al.* in 1996 [1], for application in optical communication systems. However, their work also highlighted the sensitivity of LPGs to temperature and strain induced effects, preparing the field for their use in

sensing applications [3]. Since then, the interest in long period gratings has increased, and many papers are available on this topic [4]–[7].

Nowadays, LPGs find wide application mostly as refractive index sensors [8], due to their sensitivity to the material surrounding the cladding in the grating region. Such response arises from the dependence of the resonance wavelengths on the effective refractive index of the cladding modes, as established by (1), which in turn depends upon the refractive index of the surrounding environment. Thanks to their intrinsic sensitivity to surrounding refractive index (SRI) changes, long period gratings represent one of the most promising fiber grating technological platform to be employed in several chemical applications [9], [10], with the possibility to have sensitivities custom designed to specific parameters of interest [11]. Until now, great efforts have been done, and are still in progress, in order to enhance the performance of LPGs in single mode fibers (SMFs). In particular, several approaches have been proposed to achieve remarkable sensitivities, such as: cladding etching and coupling to higher order cladding modes, near their dispersion turning point [12]–[14].

Another approach to achieve high sensitivities, involves the deposition of nano-scale high refractive index layer, thanks to the modal transition phenomenon [15], [16]. For example, in [10], a LPG was coated with syndiotactic polystyrene, to develop an high sensitivity chemical sensor. The device was able to detect chloroform subparts-per-million in water, even starting from a bare grating with refractive index sensitivity of about 5.1 nm/RIU (for LP_{06}). Similar grating was recently used in [17] to develop an high sensitive biosensor. Finally, the latest trends see the combination of all these effects, reaching record sensitivities of tens of micrometers [18]–[20].

Long period gratings are fabricated by inducing a periodic perturbation along the optical fiber, by acting on the refractive index of silica and/or on the waveguide geometry. They distinguish as "long" because the length of their period Λ is typically between 100 μm and 1 mm, being much greater than in fiber Bragg gratings (FBGs), where it is smaller than 1 μm [4]. From their first presentation, different techniques were applied for their fabrication, the most important being: UV radiation [1] [2], CO_2 lasers [21], [22], IR femtosecond lasers [23], ion implantation [24], mechanical microbends [25], and electric arc discharge [26]–[28].

The last technique, i.e., the Electric Arc Discharge (EAD), has experienced wide diffusion during the last years since it is a straight, flexible and economical step-by-step procedure. LPGs obtained via electric arc discharge were first presented by Dianov *et al.* [26]. From that work, the EAD technique has been widely investigated and review papers have been published by different researchers [29], [30]. In this technique the perturbation is created, as its name suggests, by applying an electric arc to the fiber with a certain periodicity. The formation of the grating, in most cases it is attributed to fiber geometrical changes and to silica stress relaxation, caused by the high temperature generated during the arc discharge [28], [31]. The effects of dopant diffusion and micro-deformations were also investigated in specific cases [27], [28], [32], [33]. In addition, some papers also discussed on the conditions leading to symmetry or asymmetry of cladding modes involved in the coupling mechanism in arc-induced LPGs [34], [35]. One of the most appealing feature of the electric arc discharge procedure is the intrinsic possibility to write gratings in all kind of optical fibers. In particular, there are evidences of successful fabrication in: boron co-doped fibers [36], Ge-free fibers [37], photonic crystal fibers [38]–[40], and cladding-etched fibers [12], [41], [42]. Moreover, the authors have recently successfully proposed a pressure-assisted electric arc discharge technique, to fabricate long period gratings in hollow core fibers [43]–[45] and have applied the EAD techniqu to Fluorine-doped fibers [46], [47], which are important for applications in radiation environments [48], [49].

EAD-based techniques have also some limitations, the most important being the difficulty in the fabrication of LPGs with small spatial periods, i.e. a limitation in the maximum cladding mode order. This is the reason why in recent years great efforts have been done in such direction. In 2011, Smietana *et al.* reported on the fabrication of grating in SMF28 fiber with very low period, $\Lambda = 345$ μm, as a fabrication limit of the EAD technique [50]. In 2016, the research group of Rego also investigated the realization of LPGs with period lower than 200 μm in SMF28 fiber, but with results still not satisfactory from the practical point of view; in fact, as the authors themselves declare, a

weak grating was obtained even after 400 arc discharges, with a final length of the device greater than 78 mm [13]. Differently, gratings with lower period of 221 μm and 200 μm (with a grating length greater than 50 mm) were demonstrated in a boron co-doped fiber, which is more sensitive to the arc effect than standard fiber [50], [51].

In this work, we first report on the assessment of our electric arc based system for the fabrication of LPGs in standard SMF28 fiber with period close the technique limit, representing valuable candidates for the development of chemical sensors. Thanks to the optimization of the fabrication parameters, it was possible the fabrication of gratings suitable from the practical point of view, i.e. negligible power losses, bands with depth greater than 20 dB, grating length relatively low ranging in 20-35 mm (for the investigated devices), and with a full control of the period. However, so far, there have been no general systematic experimental investigations on the chemical sensitivity of LPGs as function of the fabrication parameters. Here, for the first time to the best of our knowledge, we report a wide experimental investigation on the dependence of the surrounding refractive index sensitivity of high order cladding modes on the grating period Λ. The study allows deriving design criteria to maximize the SRI sensitivity of bare gratings.

2. Fabrication of LPGs by Electric Arc Discharge Technique

The operating principle of electric arc discharge technique involves that a certain length of optical fiber, being previously uncoated, is positioned between two electrodes. During the entire procedure, one end of the fiber is blocked on a remotely controlled precision translation stage, while the other end is kept under constant axial tension (the reason will be clear soon). In order to create the perturbation, the arc discharge is applied to a short portion of the uncoated fiber. During the process, the electrodes are supplied by an electric current of the order of mA and with duration of hundreds of milliseconds. The arc is repeated several times in order to induce a period perturbation, with the fiber axially displaced by the grating period (typically in the range 300-700 μm) between each arc, until the desired spectral features are reached [28]. The main effect of the arc discharge is twofold: i) a modification in the geometry of the optical fiber, i.e., a localized tapering of the transversal size of the core and cladding regions along the fiber and ii) a change in the silica refractive index, due to the stress relaxation induced by local hot spots [32].

The core of our computer assisted step-by-step fabrication setup for LPGs is reported in Fig. 1(a) [46]. Arc discharges are provided by the electrodes of a commercial fusion splicer (model Sumitomo Type-39), properly modified to allow the full control of the discharge parameters, and operating in the open hood mode, in order to improve the alignment of the fiber between electrodes. The selection of the power and duration of the electrodes supply current, as well as the fiber tension, allows the control of the modulation strength and thus LPG spectral features. Typical values are the arc power in range of 1-15 step (proprietary unit) and duration of 200-900 ms. In this case, a constant force of about 118 mN was applied to the fiber by using a 12 g weight and a high precision pulley. Moreover, to overcome the limitation in the minimum fabrication period, we decided to introduce another parameter in the procedure, i.e. the electrodes gap. In particular, such distance was changed from the standard value of 2.0 mm to values in range 0.8-1.8 mm, in order to decrease the fiber region affected by the discharge. The setup is completed by a micro-stepper (with resolution better than 1.0 μm) to move the fiber. Finally, the grating transmission spectra were recorded with optical spectrum analyzer (OSA) Yokogawa AQ6370B, set to a resolution of 0.1 nm, while the illumination was provided by a broadband source (SLED in range 1100-1700 nm).

For the purpose of this work, several LPGs were written in standard SMF28e optical fiber supplied by OZ Optics Ltd ($D_{core} = 8.2\,\mu$m, $D_{clad} = 125\,\mu$m, MFD $= 10.4 \pm 0.8\,\mu$m @ 1550 nm, NA $= 0.14$). The period Λ was selected in range 350-500 μm, in order to focus the attention on LP_{05} and LP_{06} attenuation bands in the wavelength range of 1100-1650 nm. The arc power was chosen in range 10-12 step and arc durations of 600-850 ms. The fabrication parameters were selected in order to compensate the ageing of the splicer electrodes and to keep the grating length lower than 35 mm in all cases. The spectra of six gratings are reported in Fig. 1(b):

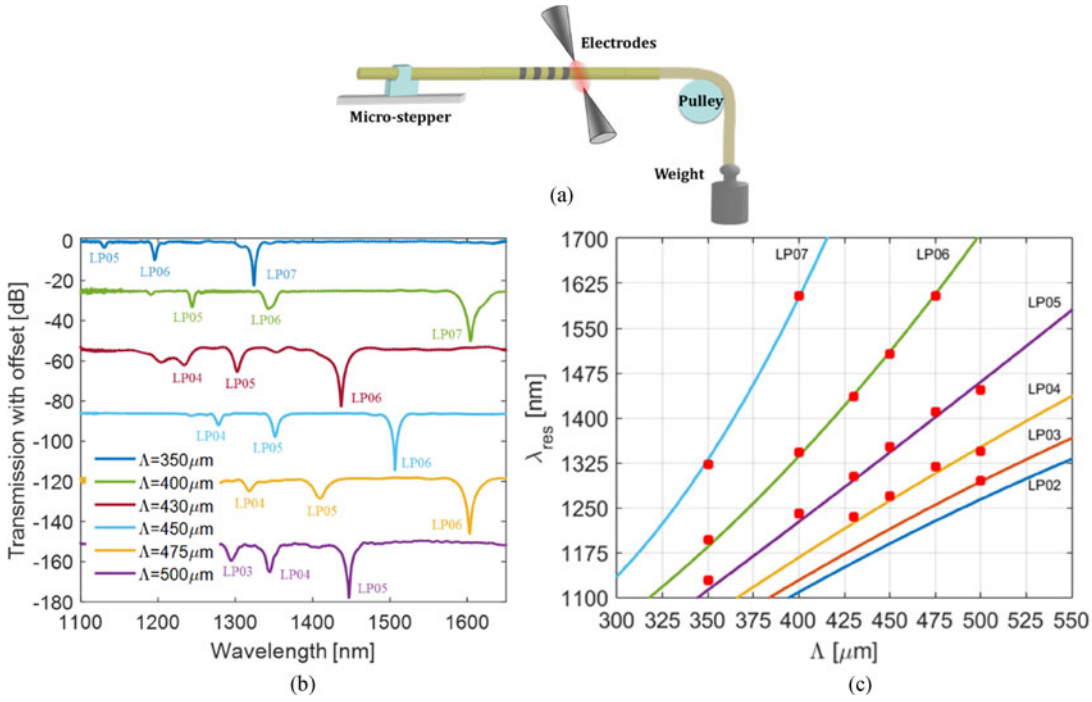

Fig. 1. a) Schematic of EAD fabrication setup. b) Transmission spectra of LPGs written in SMF28e fiber, with period Λ in range 350-500 μm. c) Phase-matching curves, comparison between numerical results (solid lines), and experimental values (markers).

i) LPG with $\Lambda = 350\,\mu$m. In the wavelength range of 1100-1650 nm, three attenuation bands are visible, centered at 1129.1 nm, 1195.5 nm, and 1323.1 nm, with depth of 3.6 dB, 9.8 dB, and 22.4 dB, respectively. From numerical simulations, we were able to associate these bands to the coupling between the fundamental core mode LP_{01} and the cladding modes LP_{05}, LP_{06}, and LP_{07} (more detailed evidence soon).
ii) LPG with $\Lambda = 400\,\mu$m. In the spectrum, three attenuation bands are centered at 1244.2 nm, 1344.3 nm, and 1604.1 nm, with depth of 8.4 dB, 9.0 dB, and 25.4 dB, respectively. Also in this case, these bands are associated to LP_{05}, LP_{06}, and LP_{07}, respectively.
iii) LPG with $\Lambda = 430\,\mu$m. Three attenuation bands are visible, centered at 1234.0 nm, 1302.6 nm, and 1437.1 nm, with depth of 8.7 dB, 12.3 dB, and 29.1 dB, respectively. In this case and for the following gratings, unless explicitly indicated, the bands are associated to the cladding modes LP_{04}, LP_{05}, and LP_{06}.
iv) LPG with $\Lambda = 450\,\mu$m. In the range reported, three attenuation bands are visible, centered at 1278.3 nm, 1350.5 nm, and 1507.6 nm, with depth of 5.4 dB, 11.5 dB, and 28.5 dB, respectively.
v) LPG with $\Lambda = 475\,\mu$m. In its spectrum, three attenuation bands are centered at 1318.0 nm, 1410.2 nm, and 1603.9 nm, with depth of 5.6 dB, 9.8 dB, and 28.0 dB, respectively.
vi) LPG with $\Lambda = 500\,\mu$m. For this grating, the LP_{04} and LP_{05} bands are positioned at 1344.0 nm and 1447.2 nm, with depth of 15.4 dB and 29.1 dB, respectively.

According to theory, attenuation bands exhibit red shifts with period increasing, justifying the necessity of smaller periods in order to excite higher order cladding modes [2], [4]. As briefly anticipated, in order to support the fabrication phase and to validate the experimental results, a numerical model for the simulation of LPGs' spectra based on the coupled-mode theory was also developed [15], [52].

The model fitting parameters for our fabrication process were identified, and an outcome is illustrated in Fig. 1(c), reporting i) as solid lines, the phase-matching curves, illustrating the resonance

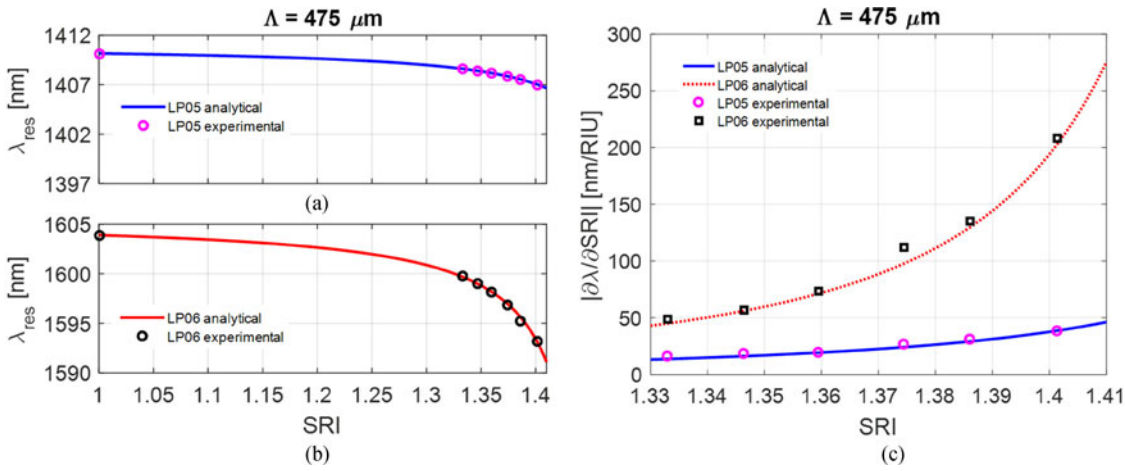

Fig. 2. LPG with $\Lambda = 475\ \mu$m versus SRI. Wavelength shift for LP_{05} (a) and LP_{06} (b) cladding modes. c) Sensitivity (absolute value) for LP_{05} and LP_{06}.

wavelengths of cladding modes $LP_{02}-LP_{07}$ versus grating period and ii) as markers, the experimental values for the LPGs reported in Fig. 1(b). As one can observe, a good agreement between experimental and numerical values was achieved, confirming the repeatability performances of our technique and allowing us the identification of the modes involved into coupling.

3. LPGs Characterization to Surrounding Refractive Index Changes

The SRI sensitivity is one of the most important feature of LPGs, in order to fabricate opto-chemical sensors. On this line of argument, after the fabrication process we investigated the sensitivity of LPGs reported in Fig. 1(b) to surrounding refractive index changes, by placing them in liquids with known RI in range 1.33-1.40. The RI of the aqueous solutions was measured with Abbe refractometer and, in addition, all the gratings were kept in the same strain state during the characterization process.

Fig. 2(a) and (b) report the wavelength shifts for LP_{05} and LP_{06} bands, respectively, concerning the LPG with $\Lambda = 475\,\mu$m, whose spectrum is reported in Figure 1(b). According to the theoretical LPG behavior, attenuation bands exhibit a blue shift with SRI increasing, with the magnitude of the shift increasing with the mode order [4], [8]. In particular, the LPG considered has a maximum wavelength shift, for LP_{05} and LP_{06} bands, respectively, of -1.5 nm and -4.1 nm, for a SRI change in the range 1-1.33, whereas in the SRI range 1-1.40 the maximum shift is -3.1 nm and -10.4 nm, for the same bands. Similar considerations hold for the other gratings, which are not reported here for brevity.

Once that all the gratings were characterized, the attention was focused on the analysis of the resonant wavelength shifts, to determine how the SRI sensitivity characteristics are influenced by the grating period.

To this aim, an analytical form was chosen to model the wavelength shift related to changes in surrounding refractive index. Each resonance wavelength $\lambda_{res,i}$ associated with the cladding mode LP_{0i} can be expressed as

$$\lambda_{res,i} = \lambda_{res0,i} \cdot \left[\frac{1 - a_i \cdot (SRI - 1)}{1 - b_i \cdot (SRI - 1)}\right] \tag{2}$$

where a_i, b_i, and $\lambda_{res0,i}$ are the fitting parameters, with the latter corresponding to the resonance wavelength value in air. These parameters depend on the cladding mode and the grating period, and their values are reported in Table 1 for LPGs under investigation. The expression of (2) was chosen in light of its simplicity and accuracy. To evaluate the latter, the fitting curves (as solid lines) were also reported, together with experimental data (markers), in Fig. 2(a) and (b).

TABLE 1
Fitting Parameter Values

Period [μm]	Cladding mode	λ_0 [nm]	a	b	S_0 [nm/RIU]
350	LP_{05}	1129.97	2.1287	2.1285	−0.1452
	LP_{06}	1195.87	2.0016	2.0007	−1.0505
400	LP_{05}	1244.46	1.8077	1.8070	−0.9453
	LP_{06}	1344.08	1.9893	1.9878	−1.9988
430	LP_{05}	1302.68	1.9772	1.9764	−1.0882
	LP_{06}	1436.57	2.0522	2.0502	−2.8748
450	LP_{05}	1348.50	1.9686	1.9677	−1.3033
	LP_{06}	1509.03	2.0201	2.0178	−3.4881
475	LP_{05}	1410.16	1.9907	1.9896	−1.5708
	LP_{06}	1603.89	2.1650	2.1628	−3.5288
500	LP_{05}	1446.07	2.0963	2.0952	−1.5906

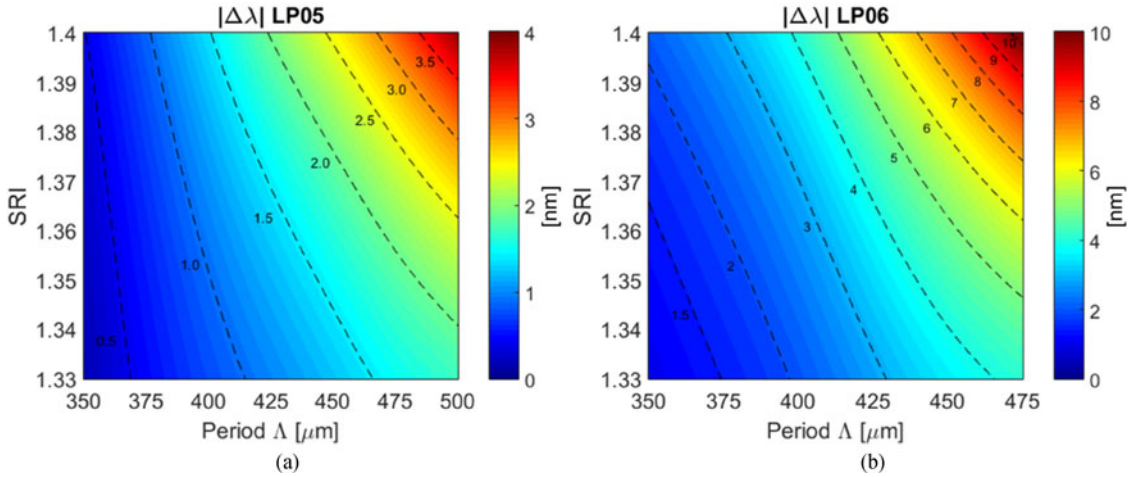

Fig. 3. Dependence of the relative wavelength shift (absolute value calculated respect to the value in air) on the period and on the SRI for LP_{05} (a) and LP_{06} (b) cladding modes.

The agreement is very strict, moreover the fitting was tested with different cladding modes and many different gratings. In particular, an average coefficient of determination $R^2 = 0.997$ was obtained for the LPGs considered in this work.

By using (2), it was possible to focus the attention on the dependence of the resonant wavelengths shifts over the grating period Λ. The modules of wavelength shifts related to LP_{05} and LP_{06} cladding modes are plotted, as color maps, versus the grating pitch and SRI in Fig. 3(a) and (b), respectively. About period, the discrete data points (related to gratings plotted in Fig. 1(b)) were interpolated with cubic spline method in order to obtain a denser interval. Concerning LP_{06}, the analysis was conducted up to $\Lambda = 475\,\mu$m, since for slightly higher periods, the band becomes no more visible in the wavelength range under investigation.

As expected from the theory, the color maps report that the wavelength shift increases with SRI and with mode order. Most important, it is also evident that focusing on a cladding mode, the shift increases with period. For LP_{05}, we calculated that wavelength shift (absolute value) passes from

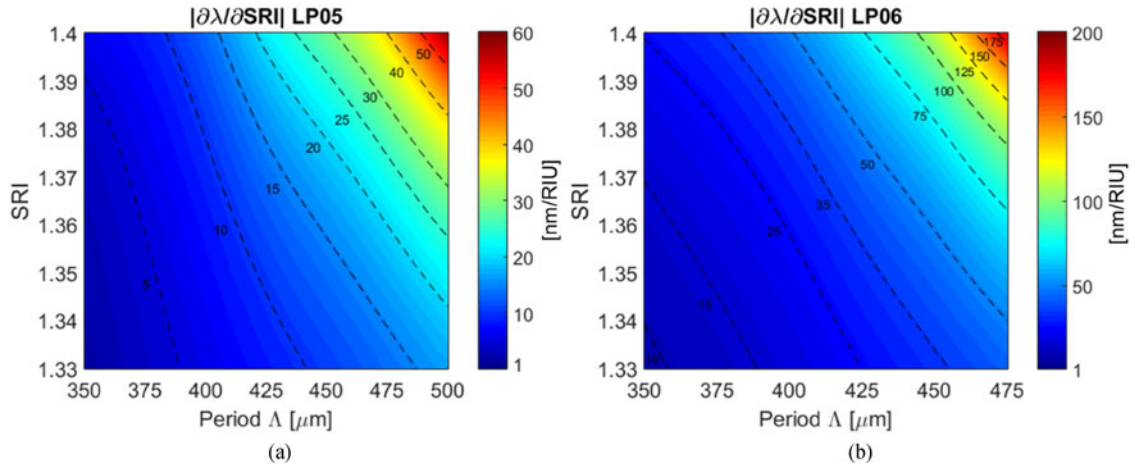

Fig. 4. Dependence of SRI sensitivity (absolute value) on the period and on the SRI for LP_{05} (a) and LP_{06} (b) cladding modes.

0.2 nm to 1.7 nm for a change in the period from 350 μm to 500 μm and with SRI = 1.33, i.e., an enhancement of 8.5. This value is bigger with higher SRI; in fact, in the same condition, the enhancement is 9.8 for SRI = 1.40, due to shift passing from 0.4 nm to 3.9 nm. Concerning LP_{06}, that wavelength shift passes from 1.0 nm to 4.1 nm for a change in the period from 350 μm to 475 μm and with SRI = 1.33 (the enhancement factor is 4.1). Also in this case, considering SRI = 1.40 the enhancement increases to 5.2, with shift passing from 2.1 nm to 10.4 nm.

4. Analysis of the LPGs' Sensitivity to Surrounding Refractive Index

Once that the wavelength shift curves were modelled, it was possible to retrieve an analytical form for the SRI sensitivity. By applying the derivative, respect to SRI, to the resonance wavelengths, the SRI sensitivity can be expressed as

$$S = \frac{\partial \lambda_{res,i}}{\partial SRI} = \frac{\lambda_{res0,i} \cdot (b_i - a_i)}{[1 - b_i \cdot (SRI - 1)]^2} = \frac{S_{0,i}}{[1 - b_i \cdot (SRI - 1)]^2}. \quad (3)$$

From this expression it is also possible to highlight the relationship between the SRI sensitivity in air S_0 and the fitting parameters a_i, b_i, $\lambda_{res0,i}$.

Fig. 2(c) illustrates the sensitivity characteristics (absolute value) of LP_{05} and LP_{06} cladding modes, respectively, for the LPG with $\Lambda = 475$ μm, obtained by using (3). In the same figure, for comparison we have reported the experimental values as markers. In particular, the estimate of the experimental sensitivity was obtained by calculating the central differences of raw data for resonance wavelengths shifts. As one can observe, good agreement was found demonstrating the suitability of the analytical form used to model both the SRI wavelength shift and sensitivity in long period gratings.

As evident, the SRI sensitivity increases with mode order and with SRI (maximum is reached for SRI values approaching the cladding RI) [4], [8]. Moreover, the achieved sensitivity values are similar (or slightly higher) with values of the bare gratings published in [10], [17] and successfully applied for chemical- and bio-sensors.

Hence, by following the same approach used in the case of wavelength shifts, it was possible to focus the attention on the dependence of the SRI sensitivity over the grating period Λ. Hence, Fig. 4(a) and (b) plot color maps of the SRI sensitivities versus grating pitch and SRI for the resonances related to LP_{05} and LP_{06} modes, respectively.

As illustrated, the sensitivity increases with mode order and with SRI. Moreover, focusing the attention on a cladding mode, the sensitivity increases also with period, as expected from

(1). For LP_{05} the absolute SRI sensitivity passes from 1.6 to 16.6 nm/RIU for a change in the period from 350 μm to 500 μm and with SRI = 1.33, i.e., a sensitivity enhancement factor of 10.4. This value is bigger with higher SRI, in fact in the same condition the sensitivity enhancement is 11.4 for SRI = 1.40, with sensitivity passing from 5.2 to 59.2 nm/RIU. Considering LP_{06}, we calculated that SRI sensitivity passes from 8.9 to 42.8 nm/RIU for a change in the period from 350 μm to 475 μm and with SRI = 1.33, i.e. a sensitivity enhancement factor of 4.8. This value becomes bigger as SRI increases, e.g. in the same condition the enhancement is 7.3 for SRI = 1.40, with sensitivity growing from 47.7 to 186.3 nm/RIU.

Hence, it was found that the SRI sensitivity is a monotonically increasing function of the grating period with superlinear behavior. It is important to highlight that the behavior illustrated here, concerning the cladding modes LP_{05} and LP_{06}, holds in similar manner for the other cladding modes, as well as the slope of their phase-matching curve is positive (i.e., before their dispersion turning point). We believe that this analysis represents a useful tool for design of LPGs aimed to chemical/biochemical sensing applications.

5. Conclusion

In this work, we have presented the assessment of our electric arc discharge based technique in order to fabricate long period gratings for chemical sensing applications, due to their appealing spectral features (e.g. negligible power losses, bands depth greater than 20 dB, and total length smaller than 35 mm) and with low period to excite high order cladding modes.

For the purpose of the work, several LPGs were fabricated with a period selected in range 350-500 μm to focus the attention on the same cladding modes (LP_{05} and LP_{06}). Then, an experimental analysis was conducted, concerning the sensitivity characteristics to surrounding refractive index changes, in order to understand the influence of the period. Such work represents a useful tool for the design of LPG with high SRI sensitivity. The enhancement in the SRI sensitivity, by acting on grating period, was shown as color map versus period and SRI. Considering LP_{06} and SRI = 1.33, the sensitivity is increased almost five times by passing from a period of 350 μm to a period of 475 μm. However, the enhancement is more than seven for SRI = 1.40. Besides, for LP_{05}, if the wider range of 350-500 μm is considered, increases in sensitivities of one order of magnitude can be also achieved.

References

[1] A. M. Vengsarkar, P. J. Lemaire, J. B. Judkins, V. Bhatia, T. Erdogan, and J. E. Sipe, "Long-period fiber gratings as band-rejection filters," *J. Light. Technol.*, vol. 14, no. 1, pp. 58–64, Jan. 1996.

[2] V. Bhatia and A. M. Vengsarkar, "Optical fiber long-period grating sensors," *Opt. Lett.*, vol. 21, no. 9, pp. 692–694, 1996.

[3] V. Bhatia, "Applications of long-period gratings to single and multi-parameter sensing.," *Opt. Exp.*, vol. 4, no. 11, pp. 457–466, 1999.

[4] S. W. James and R. P. Tatam, "Optical fibre long-period grating sensors: Characteristics and application," *Meas. Sci. Technol.*, vol. 14, no. 5, pp. R49–R61, 2003.

[5] A. D. Kersey *et al.*, "Fiber grating sensors," *J. Light. Technol.*, vol. 15, no. 8, pp. 1442–1462, Aug. 1997.

[6] S. A. Vasiliev and O. I. Medvedkov, "Long-period refractive index fiber gratings: Properties, applications, and fabrication techniques," *Proc. SPIE*, vol. 4083, pp. 212–223, 2000.

[7] A. Iadicicco, D. Paladino, P. Pilla, S. Campopiano, A. Cutolo, and A. Cusano, "Long period gratings in new generation optical fibers," in *Recent Progress in Optical Fiber Research*, Rijeka, Croatia: InTech., 2012.

[8] H. J. Patrick, A. D. Kersey, and F. Bucholtz, "Analysis of the response of long period fiber gratings to external index of refraction," *J. Light. Technol.*, vol. 16, no. 9, pp. 1606–1612, Sep. 1998.

[9] X. Shu, L. Zhang, and I. Bennion, "Sensitivity characteristics of long-period fiber gratings," *J. Light. Technol.*, vol. 20, no. 2, pp. 255–266, Feb. 2002.

[10] A. Cusano *et al.*, "Coated long-period fiber gratings as high-sensitivity optochemical sensors," *J. Light. Technol.*, vol. 24, no. 4, pp. 1776–1786, Apr. 2006.

[11] A. Cusano, A. Iadicicco, P. Pilla, A. Cutolo, M. Giordano, and S. Campopiano, "Sensitivity characteristics in nanosized coated long period gratings," *Appl. Phys. Lett.*, vol. 89, no. 20, 2006, Art. no. 201116.

[12] A. Iadicicco, S. Campopiano, M. Giordano, and A. Cusano, "Spectral behavior in thinned long period gratings: Effects of fiber diameter on refractive index sensitivity.," *Appl. Opt.*, vol. 46, no. 28, pp. 6945–6952, 2007.

[13] C. Colaco, P. Caldas, I. Del Villar, R. Chibante, and G. Rego, "Arc-induced long period fiber gratings in the dispersion turning points," *J. Light. Technol.*, vol. 34, no. 19, pp. 4584–4590, Oct. 2016.

[14] I. Del Villar, J. L. Cruz, A. B. Socorro, J. M. Corres, and I. R. Matias, "Sensitivity optimization with cladding-etched long period fiber gratings at the dispersion turning point," *Opt. Exp.*, vol. 24, no. 16, pp. 17680–17685, 2016.
[15] I. Del Villar, I. Matías, F. Arregui, and P. Lalanne, "Optimization of sensitivity in long period fiber gratings with overlay deposition," *Opt. Exp.*, vol. 13, no. 1, pp. 56–69, 2005.
[16] A. Cusano *et al.*, "Cladding mode reorganization in high-refractive-index-coated long-period gratings: effects on the refractive-index sensitivity," *Opt. Lett.*, vol. 30, no. 19, pp. 2536–2538, 2005.
[17] G. Quero *et al.*, "Long period fiber grating nano-optrode for cancer biomarker detection," *Biosens. Bioelectron.*, vol. 80, pp. 590–600, 2016.
[18] P. Pilla, C. Trono, F. Baldini, F. Chiavaioli, M. Giordano, and A. Cusano, "Giant sensitivity of long period gratings in transition mode near the dispersion turning point: an integrated design approach.," *Opt. Lett.*, vol. 37, no. 12, pp. 4152–4154, 2011.
[19] I. Del Villar, "Ultrahigh-sensitivity sensors based on thin-film coated long period gratings with reduced diameter, in transition mode and near the dispersion turning point," *Opt. Exp.*, vol. 23, no. 7, pp. 8389–8398, 2015.
[20] M. Śmietana, M. Koba, P. Mikulic, and W. J. Bock, "Towards refractive index sensitivity of long-period gratings at level of tens of μm per refractive index unit: Fiber cladding etching and nano-coating deposition," *Opt. Exp.*, vol. 24, no. 11, pp. 11897–11904, 2016.
[21] D. D. Davis, T. K. Gaylord, E. N. Glytsis, S. G. Kosinski, S. C. Mettler, and A. M. Vengsarkar, "Long-period fibre grating fabrication with focused CO_2 laser pulses," *Electron. Lett.*, vol. 34, no. 3, pp. 302–303, 1998.
[22] Y. Wang, "Review of long period fiber gratings written by CO_2 laser," *J. Appl. Phys.*, vol. 108, no. 8, 2010, Art. no. 81101.
[23] Y. Kondo, K. Nouchi, T. Mitsuyu, M. Watanabe, P. G. Kazansky, and K. Hirao, "Fabrication of long-period fiber gratings by focused irradiation of infrared femtosecond laser pulses.," *Opt. Lett.*, vol. 24, no. 10, pp. 646–648, 1999.
[24] M. Fujimaki, Y. Ohki, J. L. Brebner, and S. Roorda, "Fabrication of long-period optical fiber gratings by use of ion implantation," *Opt. Lett.*, vol. 24, no. 2, pp. 88–89, 2000.
[25] S. Savin, M. J. Digonnet, G. S. Kino, and H. J. Shaw, "Tunable mechanically induced long-period fiber gratings.," *Opt. Lett.*, vol. 25, no. 10, pp. 710–712, 2000.
[26] E. M. Dianov *et al.*, "Thermo-induced long-period fibre gratings," in *Proc. 23rd Eur. Conf. Opt. Commun.*, 1997, pp. 53–56.
[27] S. G. Kosinski and A. M. Vengsarkar, "Splicer-based long-period fiber gratings," in *Proc. Opt. Fiber Commun. Conf. Exhib.*, 1998, pp. 278–279.
[28] G. Rego, P. V. S. Marques, J. L. Santos, and H. M. Salgado, "Arc-induced long-period gratings," *Fiber Integr. Opt.*, vol. 24, nos. 3–4, pp. 245–259, 2005.
[29] S.-Y. Tan, Y.-T. Yong, S.-C. Lee, and F. A. Rahman, "Review on an arc-induced long-period fiber grating and its sensor applications," *J. Electromagn. Waves Appl.*, vol. 29, no. 6, pp. 703–726, 2015.
[30] G. Rego, "Arc-induced long period fiber gratings," *J. Sensors*, vol. 2016, 2016, Art. no. 3598634.
[31] H. S. Ryu, Y. Park, S. T. Oh, Y. Chung, and D. Y. Kim, "Effect of asymmetric stress relaxation on the polarization-dependent transmission characteristics of a CO2 laser-written long-period fiber grating," *Opt. Lett.*, vol. 28, pp. 155–157, 2003.
[32] G. Rego, O. Okhotnikov, E. Dianov, and V. Sulimov, "High-temperature stability of long-period fiber gratings produced using an electric arc," *J. Light. Technol.*, vol. 19, no. 10, pp. 1574–1579, Oct. 2001.
[33] I. K. Hwang, S. H. Yun, and B. Y. Kim, "Long-period fiber gratings based on periodic microbends.," *Opt. Lett.*, vol. 24, no. 18, pp. 1263–1265, 1999.
[34] G. Rego, O. V Ivanov, and P. V. S. Marques, "Demonstration of coupling to symmetric and antisymmetric cladding modes in arc-induced long-period fiber gratings," *Opt. Exp.*, vol. 14, no. 21, pp. 9594–9599, 2006.
[35] O. V Ivanov and G. Rego, "Origin of coupling to antisymmetric modes in arc-induced long-period fiber gratings.," *Opt. Exp.*, vol. 15, no. 21, pp. 13936–13941, 2007.
[36] M. Smietana, W. J. Bock, and P. Mikulic, "Comparative study of long-period gratings written in a boron co-doped fiber by an electric arc and UV irradiation," *Meas. Sci. Technol.*, vol. 21, no. 2, Feb. 2010, Art. no. 25309.
[37] G. Rego *et al.*, "Effect of ionizing radiation on the properties of arc-induced long-period fiber gratings.," *Appl. Opt.*, vol. 44, no. 29, pp. 6258–6263, 2005.
[38] H. Dobb, K. Kalli, and D. J. Webb, "Measured sensitivity of arc-induced long-period grating sensors in photonic crystal fibre," *Opt. Commun.*, vol. 260, no. 1, pp. 184–191, 2006.
[39] J. S. Petrovic, H. Dobb, V. K. Mezentsev, K. Kalli, D. J. Webb, and I. Bennion, "Sensitivity of LPGs in PCFs fabricated by an electric arc to temperature, strain, and external refractive index," *J. Light. Technol.*, vol. 25, no. 5, pp. 1306–1312, May 2007.
[40] W. J. Bock, J. Chen, P. Mikulic, T. Eftimov, and M. Korwin-Pawlowski, "Pressure sensing using periodically tapered long-period gratings written in photonic crystal fibres," *Meas. Sci. Technol.*, vol. 18, no. 10, pp. 3098–3102, 2007.
[41] A. Martinez-Rios, D. Monzon-Hernandez, and I. Torres-Gomez, "Highly sensitive cladding-etched arc-induced long-period fiber gratings for refractive index sensing," *Opt. Commun.*, vol. 283, no. 6, pp. 958–962, 2010.
[42] M. Z. R. M. Zulkifly, F. A. Rahman, and H. Y. Wong, "Arc-induced long period fiber gratings (LPFG) characterization: Comparison between cladding etched and non-etched LPFG," in *Proc. Int. Conf. Photon.*, 2010, pp. 1–3.
[43] A. Iadicicco, S. Campopiano, and A. Cusano, "Long-period gratings in hollow core fibers by pressure-assisted arc discharge technique," *IEEE Photon. Technol. Lett.*, vol. 23, no. 21, pp. 1567–1569, 2011.
[44] A. Iadicicco, R. Ranjan, and S. Campopiano, "Fabrication and characterization of long period gratings in hollow core fibers by electric arc discharge," *IEEE Sens. J.*, vol. 15, no. 5, pp. 3014–3020, May 2015.
[45] A. Iadicicco and S. Campopiano, "Sensing features of long period gratings in hollow core fibers," *Sensors*, vol. 15, no. 4, pp. 8009–8019, 2015.
[46] R. Ranjan, F. Esposito, A. Iadicicco, A. Stăncălie, D. Sporea, and S. Campopiano, "Comparative study of long period gratings written in standard and fluorine-doped fibers by electric arc discharge," *IEEE Sens. J.*, vol. 16, no. 11, pp. 4265–4273, Jun. 2016.

[47] R. Ranjan, F. Esposito, A. Iadicicco, A. Stăncălie, D. Sporea, and S. Campopiano, "Long period gratings written in fluorine-doped fibers by electric arc discharge technique," in *Proc. SPIE 6th Eur. Workshop Opt. Fibre Sensors*, 2016, vol. 9916, pp. 991622-1–991622-4.
[48] D. Sporea, A. Stancalie, D. Negut, G. Pilorget, S. Delepine-Lesoille, and L. Lablonde, "Online tests of an optical fiber long-period grating subjected to gamma irradiation," *IEEE Photon. J.*, vol. 6, no. 6, Dec. 2014, Art. no. 0600211.
[49] G. Berruti *et al.*, "A comparative study of radiation-tolerant fiber optic sensors for relative humidity monitoring in high-radiation environments at CERN," *IEEE Photon. J.*, vol. 6, no. 6, Dec. 2014, Art. no. 0601015.
[50] M. Smietana, W. J. Bock, P. Mikulic, and J. Chen, "Increasing sensitivity of arc-induced long-period gratings—Pushing the fabrication technique toward its limits," *Meas. Sci. Technol.*, vol. 22, 2011, Art. no. 15201.
[51] A. K. Debowska, M. Smietana, P. Mikulic, and W. J. Bock, "High temperature nano-coated electric-arc-induced long-period gratings working at the dispersion turning point for refractive index sensing," *Jpn. J. Appl. Phys.*, vol. 53, no. 8, SPEC, 2014, Art. no. 08ME01.
[52] E. Anemogiannis, E. N. Glytsis, and T. K. Gaylord, "Transmission characteristics of long-period fiber gratings having arbitrary azimuthal/radial refractive index variations," *J. Light. Technol.*, vol. 21, no. 1, pp. 218–227, Jan. 2003.